PHYSICAL REVIEW B **80**, 224504 (2009)

Kinetic magnetism and orbital order in iron telluride

Ari M. Turner,[1] Fa Wang,[1,2] and Ashvin Vishwanath[1,2]
[1]*Department of Physics, University of California at Berkeley, Berkeley, California 94720, USA*
[2]*Materials Sciences Division, Lawrence Berkeley National Laboratory, Berkeley, California 94720, USA*
(Received 20 July 2009; published 10 December 2009)

Iron telluride (FeTe), a relative of the iron-based high-temperature superconductors, displays unusual magnetic order and structural transitions. Here, we explore the idea that strong correlations may play an important role in these materials. We argue that the unusual orders observed in FeTe can be understood from a picture of correlated local moments with orbital degeneracy, coupled to a small density of itinerant electrons. A component of the structural transition is attributed to orbital, rather than magnetic ordering, introducing a strongly anisotropic character to the system along the diagonal directions of the iron lattice. Double exchange interactions couple the diagonal chains leading to the observed ordering wave vector. The incommensurate order in samples with excess iron arises from electron doping in this scenario. The strong anisotropy of physical properties in the ordered phase should be detectable by transport in single domains. Predictions for ARPES, inelastic neutron scattering and hole/electron doping studies are also made.

DOI: 10.1103/PhysRevB.80.224504 PACS number(s): 75.50.Ee, 74.70.−b, 71.10.−w, 71.70.Ej

I. INTRODUCTION

The discovery of high-temperature superconductivity in a class of iron based materials[1] has opened a new route to high-temperature superconductivity besides the ones operating in the copper oxide materials. Following the initial discovery in LaOFeAs (1111 materials), a number of classes of materials were discovered that shared similar properties, notably the 122 materials (such as $BaFe_2As_2$). In these systems, (collectively referred to as the FeAs materials) the undoped compound is a metallic spin density wave (SDW) system, with ordering wave vector $(\pi,0)$, which on doping leads to a superconducting state. The magnetism in these materials is believed to arise from Fermi surface nesting, given the presence of an electron and hole pocket separated by $(\pi,0)$ in the local density approximation (LDA) band structure calculations of these materials. In fact, theoretical studies had predicted this ordering before it was confirmed in neutron scattering experiments. Moreover, the typically small ordering moment, e.g., about $0.3\mu_B$ in LaOFeAs, and the absence of a Curie-Weiss form of magnetic susceptibility above the ordering temperature have been invoked as evidence for the itinerant character of the magnetism. Finally, signatures of an excitation gap appear in optical conductivity experiments, on cooling through the SDW transition.[2]

An important recent development has been the discovery of superconductivity in another class of materials, FeSe and FeTe, which share the square lattice Fe structure of the FeAs materials and are believed to be closely related. Indeed, superconductivity has been observed in FeSe even in the absence of doping at 8 K, rising to 37 K on application of hydrostatic pressure. The chemical simplicity of these materials, as well as the absence of a pnictide group element, may offer valuable clues to isolating the physics of the iron-based high-temperature superconductors. One notable difference from the FeAs materials though, is in the magnetism. While FeSe is nonmagnetic even at stoichiometry, the FeTe materials are magnetically ordered metals, but with a more complicated kind of order than seen in FeAs, shown in Fig. 1. The ordering wave vector is $(\pi/2,\pi/2)$, in contrast to the $(\pi,0)$ ordering of the FeAs compounds and also the (π,π) ordering of the insulating parent compound of the cuprate superconductors. (*Note:* the wave vectors here are defined with respect to an unfolded zone corresponding to a unit cell of one iron atom, and oriented along the iron square lattice. The actual basis vectors are $\hat{\mathbf{x}}\pm\hat{\mathbf{y}}$ because of the alternating positions of the tellurium ions; therefore, crystallographic studies use a doubled-unit cell, and a and b are along the diagonals of the iron lattice.) The order sets in via a first order

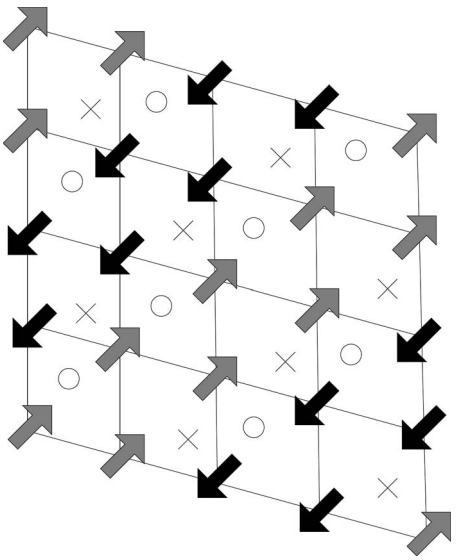

FIG. 1. The commensurate $(\frac{\pi}{2},\frac{\pi}{2})$ spin ordering pattern of $Fe_{1+x}Te_1$, close to $x=0$. The spins reside on the iron atoms, which form a square lattice. The tellurium atoms alternate above (x's) and below (o's) the iron plane. When the spins order, the square lattice of irons distorts into an approximately rhombic lattice. We assume that the monoclinic distortion is a consequence of the spin ordering. The tellurium atoms move toward (or away from) the exceptional iron spin in each parallelogram. Thus, the planes of tellurium atoms shift in opposite directions, producing the monoclinic distortion.

transition at 87 K, and is accompanied by a monoclinic distortion.[3] In the presence of excess iron, i.e., $Fe_{1+y}Te$, the commensurate order is found to evolve into an incommensurate spiral.[4] Whether this complex magnetic behavior is important to understanding other physics in this material is presently unclear. So far, it is unique to FeTe, where superconductivity only occurs on substantial alloying with sulfur $FeS_{0.2}Te_{0.8}$ or selenium $FeSe_{0.5}Te_{0.5}$. However, besides the interest in understanding the origin of this unusual magnetism, there are a number of indicators that point to the presence of strong correlations in FeTe, which would be an important fact to establish in these materials. (1) The ordered magnetic moment in the commensurate phase of FeTe is large, $\sim 2\mu_B$,[5] consistent with a localized $S=1$ at every site. (2) Above the ordering temperature the magnetic susceptibility falls off in a Curie Weiss fashion,[6] roughly consistent with the observed ordered moment and transition temperature,[7] (3) given the absence of Fermi surface nesting at this wave vector,[8] a spin-density wave scenario seems less favorable than a local moment picture. Furthermore, ARPES (angle resolved photoemission spectroscopy) experiments on this material see no obvious nesting at the desired wave vector,[9] and (4) optical conductivity, which observes a clear SDW gap in the FeAs materials, does not see an analogous gap in FeTe.[10] Another mechanism is therefore needed to explain the peculiar spin ordering. Here, we will assume that the magnetism in FeTe arises from local magnetic moments on the iron sites, that arise from strong correlations. However, given that FeTe is metallic [with a residual resistivity of 0.2 $m\Omega$ cm (Ref. 10)], we will have to consider them as being "self-doped." The key point of this paper is that several of the puzzling magnetic properties of FeTe can be naturally explained if we assume it is near a correlated insulating state with spin and orbital degeneracies. Furthermore, the structural distortion here will be explained as arising, at least partially, from orbital ordering, rather than spin lattice interaction as is usually assumed. A model for FeTe's ordering, in which the lattice distortion is assumed from the outset is in Ref. 11. Other scenarios based on an itinerant electron picture have also been put forward,[12] such as the possibility that electron doping is large enough to change the Fermi surface shape and lead to nesting.[13]

The main assumptions we make in this paper are: (i) FeTe is proximate to an $S=1$ magnetic insulator. (ii) Each site of this insulator has orbital degeneracy (d_1,d_2) and the Jahn Teller effect leads to orbital ordering, which orients the orbitals along the diagonal direction of the Fe lattice. The orbital d_1 accommodating the local moment is uniformly oriented on all sites. (iii) A small excess density of charge carriers is present in the other Jahn Teller orbital d_2.

From these assumptions we show that the $(\pi/2,\pi/2)$ magnetic order can be naturally explained, as well as the incommensuration induced by excess iron. The key mechanisms are the formation of one dimensional chains induced by the Jahn Teller ordering, which are coupled together by double exchange. Part of the structural transition in this scenario is caused by orbital rather than spin ordering. Since this proposal invokes an intertwining of the spin, charge, and orbital physics, several testable consequences also emerge for transport and ARPES experiments. For example, transport within a single domain is expected to be highly anisotropic, with larger conductivity along the *ferromagnetically* ordered diagonal directions. This can potentially be probed by optical conductivity experiments. Indeed, a number of anomalies are already observed in transport properties, albeit in multidomain samples. The electrical conductivity rises sharply below the ordering transition while the Hall effect abruptly changes sign.[10]

Recently, a similar scenario has appeared to explain the magnetism and structural transition in FeAs.[14–16] In contrast to our assumption (ii), the Jahn Teller orbitals are assumed to order along the lattice directions. The spin wave spectrum experimentally observed in FeAs was argued to be described well by such a model.[15] Here, we focus on FeTe, for the reasons described previously, but our approach is very similar in spirit. If indeed this mechanism is more general, it allows us to unify phenomena across this family of compounds.

This paper is organized as follows. We first describe microscopic strongly correlated models for FeTe, which have $S=1$ and orbital degeneracy. We then consider how orbital ordering of a particular kind together with a small conductivity can drive magnetism, leading to the observed spin order. The characteristics of spin-wave dispersion within this scenario are presented, and the origin of incommensurate magnetism with excess iron, is discussed. Finally, experimental consequences of this scenario for nonmagnetic properties, such as conductivity and ARPES, are described.

II. FeTe: A STRONGLY CORRELATED VIEWPOINT

A. Microscopic model

We first model FeTe in terms of a nearby correlated insulating state. The modifications required to account for metallic conduction are discussed later. We demand that the insulator carries net spin $S=1$, per Fe atom, based on the ordered moment observed at low temperatures. Furthermore, we will require that they exhibit orbital degeneracy. The only pair of d orbitals that are degenerate in this tetragonal structure are the d_{xz} and d_{yz} orbitals. Hence, our theory depends upon having an odd filling of this orbital pair. Two possible microscopic scenarios for the d^6 configuration of the Fe^{+2} ion are sketched in Fig. 2. In the first, there is one electron available to occupy the two degenerate orbitals, while the orbital d_{xy} is singly occupied. Interestingly, this is the orbital configuration suggested by the crystal field splitting of the Fe sites. For a perfect tetrahedral arrangement of Te ions, the $d_{x^2-y^2}$ and d_{z^2} orbitals lie below the triplet of d_{xy},d_{xz},d_{yz}. The distortion of the tetrahedron in this material brings the d_{xy} below the degenerate d_{xz},d_{yz}, leading to the orbital structure in Fig. 2. Note, the sense of the distortion in FeTe is opposite to that in FeAs, where a similar exercise leads to a different orbital ordering.[4] Since such a local picture of electronic orbitals may not capture the physics of FeTe we also point out a different scenario [Fig. 2(b)], where the orbital ordering is closer to what is predicted by the band structure calculations in FeAs.[17] If we order the dispersing bands by their center of mass, we end up with the ordering shown. Here too, the electron assignment can lead to a $S=1$ orbitally degenerate

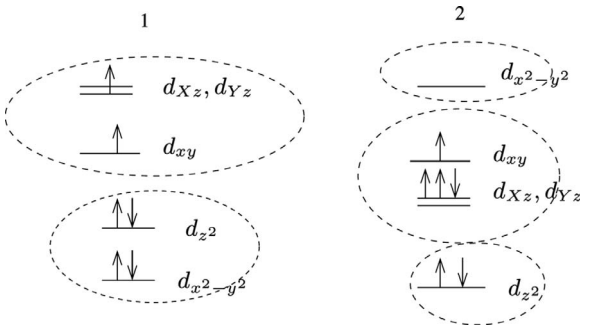

FIG. 2. Two scenarios for the level spacing of the iron atoms' d-orbitals which lead to orbital degeneracy and $S=1$. Each set of orbitals grouped together is assumed to fill up according to Hund's rule before any electrons are added to the next group of orbitals. This occurs if the crystal field splitting between orbitals in different groups is greater than the Hund's coupling. Scenario 1 results in a single electron having to decide between two degenerate orbitals while Scenario 2 results in a single hole which is orbitally degenerate. We mainly discuss Scenario 1.

configuration, but now the degenerate pair of orbitals contains three electrons. We note that in both scenarios, the active orbitals are d_{xy}, d_{xz}, d_{yz}, which are also the ones expected to be present at the Fermi energy from weakly correlated band structure calculations of these materials.[17,18] The two scenarios are particle hole conjugates of one another, if one focuses on the active triplet of orbitals. Henceforth, we will assume Scenario 1 for concreteness, as it corresponds better with experimental facts. The results there can be easily transcribed to Scenario 2, by a particle hole transformation.

B. Orbital and magnetic order

Let us discuss first the pair of degenerate orbitals in Scenario 1, filled by a single electron. Later, we will include the third orbital. It is convenient to rotate orbitals by 45°, and define another basis that point along the diagonals $d_{Xz/Yz} = \frac{1}{\sqrt{2}}(d_{xz} \pm d_{yz})$. Let $d_1^\dagger, d_2^\dagger$ be the creation operators for electrons in these diagonal orbitals. The Hamiltonian for this system is:

$$H = H_{\mathrm{KE}} + H_U + H_{JT}, \tag{1}$$

where the first term is the hopping Hamiltonian, and the second and third terms refer to interactions and coupling to lattice phonons that lead to the Jahn Teller effect.

$$H_U = \sum_r \frac{1}{2} U(n_r - 1)n_r - J_H \vec{S}_{1r} \cdot \vec{S}_{2r}, \tag{2}$$

where n_r is the electron density at site r and $\vec{S}_{ar} = \frac{1}{2} d_{ar}^\dagger \vec{\sigma} d_{ar}$ is the spin on site r in orbital a. In the limit of strong repulsion U and a single electron per site, $\langle n \rangle = 1$, we obtain an insulating state with orbital degeneracy. This degeneracy is typically resolved by the Jahn Teller effect. A lattice distortion, which breaks symmetry and splits the degeneracy occurs. The precise distortion that is realized is hard to predict, so we will assume that it is indeed of the type required to obtain the structural transition seen in this material. This involves a uniform orthorhombic distortion that changes the relative lengths of the two diagonal bonds. If we denote by A and B the classical bond lengths for the two diagonals (so $A=B$ in the tetragonal state), then we will assume that the lattice coupling is given by:

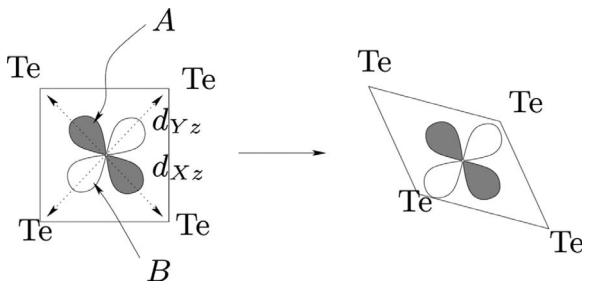

FIG. 3. Degeneracy lifting by Jahn Teller distortion. The tellurium atoms projected into the xy-plane form a square in the undistorted compound, which distorts into a rhombus, so that $A > B$, lowering the energy of the shaded orbital.

$$H_{JT} = -\alpha(A-B)\sum_r (d_{1r}^\dagger d_{1r} - d_{2r}^\dagger d_{2r}) + \frac{\beta}{2}(A-B)^2 \tag{3}$$

(See Fig. 3). The orbital ordering implies that, in scenario 1, the single electron on each site always occupies the same orbital, i.e., $n_{1r}=1$ and $n_{2r}=0$, or vice versa. For concreteness let us suppose that the X diagonal expands. Then the electrons occupy orbital 1 (d_{Xz}) while orbital 2 (d_{Yz}) is empty, because it is higher in energy. Since each site has an unpaired electron, we can now derive the Hamiltonian governing their magnetic moments.

In the insulating limit, the magnetic interaction is generated by virtual hopping of electrons. To proceed, we need to specify H_{KE}. Clearly, given the geometry of the Xz, Yz orbitals, hopping along the diagonals will be very anisotropic. We denote the $X(Y)$ diagonal hopping of the $d_{Xz}(d_{Yz})$ orbital by t_2, and let t_2' be the hopping of each in the orthogonal direction (see Fig. 4). The figure suggests that $t_2 \gg t_2'$ (see Ref. 19), and for FeAs the nearest neighbor hoppings are comparatively small as well. Hence, we will simply work with the exchange interaction induced by t_2. Note, the next neighbor hopping only operates within a single sublattice (labeled A and B in the figure), so here we consider just the A sublattice. The t_2 hopping of the electrons in the Xz orbital will introduce antiferromagnetic exchange, but only along the X diagonal $J_{2X} = t_2^2/U$. This will lead to antiferromagnetic order along this diagonal direction. Note, assuming Scenario 1, this antiferromagnetic direction will be the expanded diagonal of the distorted compound, which is consistent with the observed wave numbers of the magnetic and structural distortions.[4] Note, although the diagonal chains are ordered, there is negligible coupling between chains at this moment (because of the smallness of t_2'). Below, we will see there is a possibly more important mechanism that can lock the magnetic order in the chains together, the double exchange interaction.

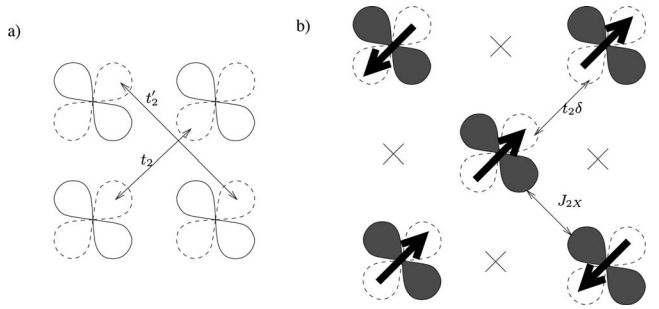

FIG. 4. How the spin-order on sublattices arises out of the orbital order. The solid and dotted lines show the projections of the d_{Xz} and d_{Yz} orbitals. (a) The second nearest neighbor hopping amplitudes, which determine the order in the sublattices. Electrons stay in the same orbital when they hop to the second nearest neighbor. The hopping for each orbital is anisotropic, with an anisotropy that depends on the orbital, so each orbital forms a set of one-dimensional chains. Electrons can hop between nearest neighbors as well (not shown). (b) Generating the spin order in the A-sublattice. (The iron atoms in the B-sublattice are indicated by x's.) The d_{Xz} orbitals are shaded to indicate that they are filled and the d_{Yz} orbitals are lightly doped. The d_{Xz} orbitals form one-dimensional Mott insulators parallel to the X-axis with antiferromagnetic coupling J_{2X}. The d_{Yz} orbitals form one-dimensional metals parallel to the Y direction. Ferromagnetic order along Y lowers the kinetic energy of the metals by about $t_2\delta$.

C. Double exchange

Hopping of electrons between the antiferromagnetic chains can readily occur if they occupy the d_{Yz} orbital. However, in an orbitally ordered insulator, these are assumed to be empty. Given the empirical fact that FeTe is a metal, we assume a small occupation δ of electrons in this orbital. This can arise because of "self-doping," i.e., if the orbital dispersion cannot be completely neglected, a fraction of carriers from one of the "filled" bands (for example d_{xy}), could be transferred to an empty band, i.e., this orbital. In addition to the self-doping, FeTe always occurs with a slight excess of Fe i.e., $Fe_{1+y}Te$. The electrons from the additional Fe^{+2} ions also contribute to δ.

Such an excess carrier density will lead to ferromagnetic interactions between chains, via the double exchange mechanism. An electron hopping in this nearly empty orbital will be Hund's coupled to the d_{Xz} electron according to Eq. (2). The Hund's coupling is typically large and will force both electrons to have the same spin. If the electron is to hop to the neighboring chain, the spins must be parallel. Then, it can enjoy a lowering of kinetic energy by $-2t_2$. Thus, a ferromagnetic arrangement of spins will have a lower energy than an antiferromagnetic arrangement by an amount $2|t_2|\delta$, which can roughly be viewed as a ferromagnetic coupling along the Y diagonal (strictly speaking this is a nonlocal interaction, and cannot be assigned solely to the diagonal bond). Thus, $J_{2Y}=-2|t_2|\delta$. The coupling J_{2X} along the X direction remains antiferromagnetic. The double-exchange along X generated by the holes left behind in the donor xy-orbitals would be negligible if the effective mass for their motion turns out to be large enough. With this combination of exchange constants, the magnetic ordering on a single sublattice is shown in Fig. 4. Note that it has the wave vector $(\pi/2,\pi/2)$, as required.

D. Coupling the sublattices

So far, the two sublattices (A and B) are independent. When the doping is small, the dominant spin interaction J, between nearest neighbor sites will arise from antiferromagnetic exchange from the electrons in the half filled d_{xy} orbital. (The nearest neighbor hopping of electrons in the d_{Xz} orbitals would induce a smaller ferromagnetic interaction controlled by the Hund's coupling, since the dominant hopping is expected to move them to d_{yz} orbitals after a hop.) We will also invoke a coupling to the lattice to generate a biquadratic interaction term in order to lock in the commensurate wave number, leading to the net Hamiltonian describing the interaction of spin 1 atoms on a square lattice:

$$H=\sum_{ij} J_{ij}\mathbf{S}_i\cdot\mathbf{S}_j - K\sum_{\langle ij\rangle}(\mathbf{S}_i\cdot\mathbf{S}_j)^2. \tag{4}$$

$J_{2X}=t_2^2/U$, $J_{2Y}=-2|t_2|\delta$ and $J_1>0$, and J_1 is the same for both nearest-neighbor bonds. The phase diagram of this model as a function of increasing K is included on the y-axis of Fig. 6. The $\mathbf{S}_i\cdot\mathbf{S}_j$ terms alone would lead to an incommensurate spiral state,[20] where the nearest neighbor spins are close to being orthogonal to one another (this is called the "single spiral state" below). This state, even in the small incommensuration limit, is significantly different from the experimentally observed collinear state.

To stabilize the commensurate $(\frac{\pi}{2},-\frac{\pi}{2})$ state, we take into account the biquadratic spin interaction $(-K(\mathbf{S}_1\cdot\mathbf{S}_2)^2)$, which is a well-known consequence of spin-lattice coupling. This term prefers collinear magnetism. As we will see below, even modest values of the spin phonon coupling K can induce locking of the commensurate, collinear phase observed in experiments. In particular, we show below that the critical coupling required to induce collinear order $K\gtrsim J_1^2/J_{2X}$ can be parametrically smaller than J_1. Coupling of spin and lattice is presumably essential to getting a commensurate state at this wave vector.

Phase Diagram: The phase diagram can be obtained by taking the ansatz of a pair of coplanar spirals on the two sublattices with an arbitrary phase ϕ between them, and wave vector k along diagonal X. This is probably sufficiently general to capture the ground states of Eq. (4), because the ferromagnetic coupling along the Y-direction prevents the spin from varying in that direction. Let the azimuthal angle of spin i be θ_i. Then the ansatz reads:

$$\theta_i=k(x_i-y_i)+(-1)^{x_i+y_i}\frac{\phi}{2}. \tag{5}$$

Here, $(k,-k)$ is the wave number of the spin arrangement. (This state is ICA, from Ref. 11.) Note, the experimentally observed collinear state corresponds to $k=\pi/2$ and $\phi=\pi/2$. Along any row, the angle between adjacent spins alternates between $k-\phi$ and $k+\phi$. For $k=\phi=\pi/2$, the spins therefore alternate from parallel to antiparallel.

Minimizing the energy per site,

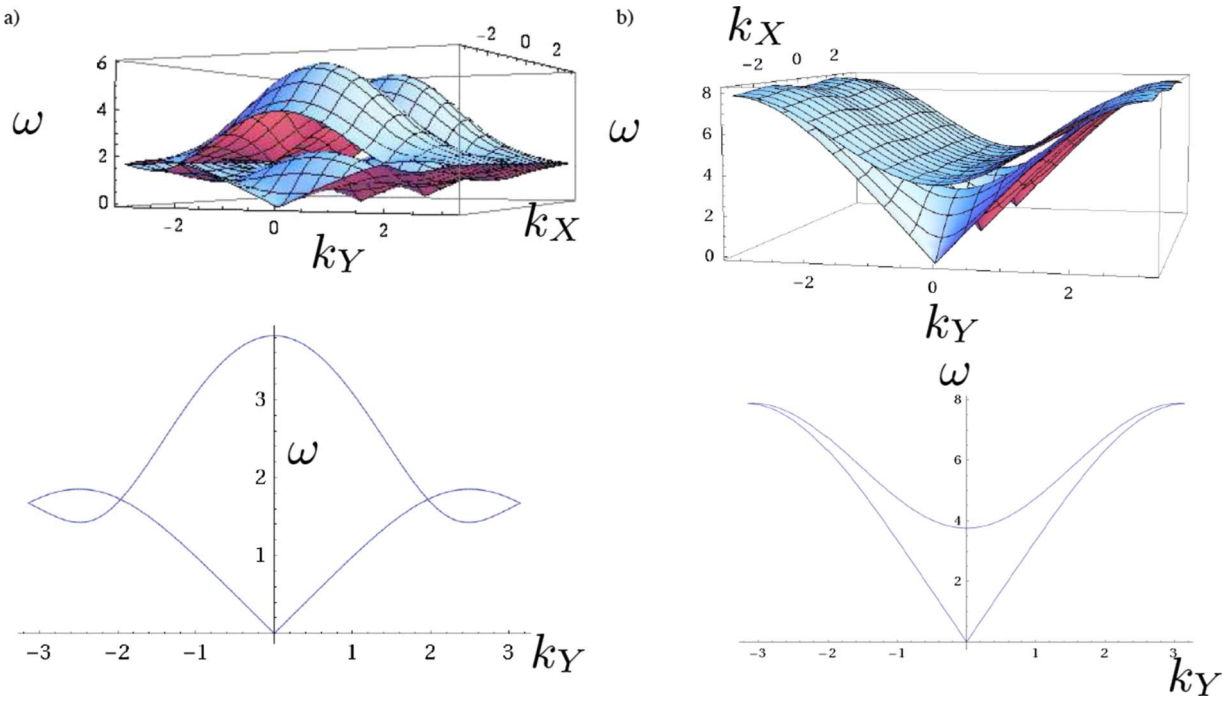

FIG. 5. (Color online) Comparison of the spin wave dispersion for order stabilized by J_3 versus by a ferromagnetic diagonal interaction. The dispersions are plotted as a function of $(k_X,k_Y)=(k_x-k_y,k_x+k_y)$ in the upper pictures. The other graphs show the dispersion in the Y direction. (a) The spin wave spectrum for $J_{2X}=J_{2Y}=1, J_1=1.47, K=0.265, J_3=0.4$, which have the same effective $J_{1w,s}$ as in Ref. 11. (b) This shows the spectrum for $J_{2X}=-J_{2Y}=1, J_1=0.7, K=0.265, J_3=0$. The sign of J_{2Y} is flipped to describe a ferromagnetic coupling, while J_3 is set to zero. [J_1's value is decreased relative to (a) to stabilize the order.] Note that the upper band changes from a hill shape to a valley.

$$E[k,\phi] = J_{2X}\cos 2k + 2J_1\cos k\cos\phi - K(1+\cos 2k\cos 2\phi) - 2|t_2|\delta \qquad (6)$$

over ϕ and k shows that there is a transition between a "single spiral" with $\phi=0$ and incommensurate wave vector $k=\frac{\pi}{2}+O(\frac{J_1}{J_{2X}})$ and the collinear state $k=\pi/2, \phi=\pi/2$ when $4K(J_{2X}-K)=J_1^2$. For small $K \ll J_{2X}$, the critical K is $\approx J_1^2/4J_{2X}$.

We can understand this result intuitively as follows. The spiral order occurs to lower the nearest neighbor exchange energy. The coupling of a spin to its neighbors to the left and right cancels in the perfectly collinear state. To take advantage of J_1, the neighbors should therefore make an angle less than 180°, and the central spin should point opposite to the sum of the two neighboring spins. If J_1 is small compared to J_{2X}, then the neighbors are *nearly* antiparallel, so J_1 has a very weak effect, explaining why the critical value for K is not of order J_1 as one might have expected, but rather second order in J_1.

Spin Waves: To contrast this scenario with others that predict the same magnetic ordering pattern, we calculate the spin wave spectrum for the model Eq. (4). We expect inelastic neutron scattering experiments in the future to be able to check this prediction. In particular, we contrast it with a recent theory,[11,21] in which there is a sufficiently large third neighbor exchange J_3 and the monoclinic distortion alters the first and second nearest neighbor interactions, leading to the observed magnetic order. In our model, the magnetic order is stabilized just by the anisotropy of J_2, with one ferromagnetic and one antiferromagnetic direction. (Refs. 11 and 21 also include the anisotropic couplings but their third neighbor hopping is essential for stabilizing the order without ferromagnetic directions.) Note, while doing the spin-wave calculations, we expand about the equilibrium spin state, and hence, the biquadratic interaction effectively leads to weak (w) and strong (s) nearest-neighbor bonds, $J_{1s} \neq J_{1w}$. That is, our spin wave dispersion is reproduced by a model involving only quadratic spin couplings, where $J_1\mathbf{S}_1\cdot\mathbf{S}_2 - K_1(\mathbf{S}_1\cdot\mathbf{S}_2)^2 \Rightarrow (J_1 - 2K_1\langle\mathbf{S}_1\cdot\mathbf{S}_2\rangle)\mathbf{S}_1\cdot\mathbf{S}_2$. Therefore, the bonds between parallel spins are effectively weaker than those between antiparallel spins, similar to Refs. 11 and 21. The spin-wave spectrum is obtained using the Holstein-Primakoff expansion (see e.g. Ref. 22). Figure 5 compares the dispersions one expects in the two models, the first with a strong J_3 and ours with a ferromagnetic diagonal coupling. Note, the upper band of the dispersions curves in the opposite direction along the Y-axis, because of the ferromagnetic coupling J_{2Y}.

E. Doping induced incommensuration

The properties of $Fe_{1+y}Te$ have been experimentally investigated as y is varied. Experimentally, $Fe_{1+y}Te$ is found to have incommensurate spin order when y is large enough, with an incommensurate wave vector that deviates from $(\pi/2,\pi/2)$ linearly with doping.[4] One of the effects of the excess iron, which is believed to be in the Fe^{2+} state, is to electron dope the system by $2y$ electrons. Here, we consider how this may be explained as a result of the increasing elec-

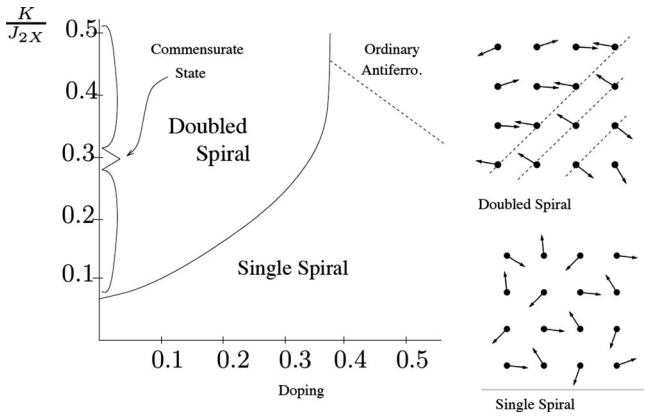

FIG. 6. The phase diagram as a function of K and doping for $J_1=\frac{1}{2}J_{2X}$, $t_2'=1.5J_{2X}$, using the infinite Hund's coupling approximation. The three phases are the doubled spiral, the single spiral, and ordinary (π,π) antiferromagnetism. Note that both the single and doubled spirals are constant along wave fronts parallel to Y. In the perpendicular direction, the double spiral alternates between rotating through small angle and angles close to 180°, while the single spiral rotates through around 90° each time. A calculation which takes fluctuations or the finiteness of the Hund's constant into account would find a finite range of dopings where the commensurate phase is stable. The solid/dashed line represents a discontinuous/continuous transition. The discontinuous transition boundary should actually be replaced by a wide swath of phase separation.

tron density $\delta=2y$ in the Yz orbital, which makes nearest neighbor hopping more important. This will lead to incommensurate order that is related to the doping level.

To see this, we will consider two-dimensional motion of the doped electrons, which can occur only if hopping amplitudes other than t_2 are taken into account. These types of motion are limited to the diagonal stripes of similarly oriented spins in the commensurate $(\frac{\pi}{2},\frac{\pi}{2})$ spin pattern, increasing the kinetic energy, according to the uncertainty principle. Such a kinetic energy effect has a stronger dependence on the relative angle between a pair of spins when the angle is close to 180° than the J_{2X} interaction considered above, so it is able to distort the commensurate collinear state with wave vector $(\frac{\pi}{2},-\frac{\pi}{2})$ and $\phi=\pi/2$, into a "*double spiral*," a slightly twisted version of the same state, of the form Eq. (5), and with $\phi\approx\frac{\pi}{2}$ and $k\approx\frac{\pi}{2}$, even when the doping is weak.

To understand the kinetic energy effect, we assume a *uniformly* varying classical spin configuration and minimize the energy of a single Hund's coupled electron, Eq. (2), hopping in this background. The resulting kinetic energy ($\mathrm{KE}_{\min}$) times electron density, $\mathrm{KE}_{\min}\delta$ is added to the magnetic energy Eq. (4), and this total energy is minimized to obtain the phase diagram in Fig. 6. A shortcoming of this phase diagram is that the spiral phases may not be stable against phase separation (see below).

We will now focus for simplicity on determining the kinetic energy due to hopping via t_2'. We checked also that the nearest neighbor t_1 of Ref. 19 leads to a very similar phase diagram. The kinetic energy is computed from the hopping Hamiltonian $H_{t_2'}=-t_2'\Sigma_i d_{Yz}^\dagger(\mathbf{r}_i+\hat{\mathbf{x}}-\hat{\mathbf{y}})d_{Yz}(\mathbf{r}_i)+\mathrm{H.c.}$, which favors ferromagnetic alignment along the X-diagonal. Since the Hund's energy is larger than the t's, the natural basis for spin states on each site are the states quantized along the local spin orientation of the magnet (θ_i). If the Hund's energy is assumed to be infinite, we can assume that the electron state is always aligned with the local spin. Such a state with momentum $\mathbf{p}$ is represented by the following electron-wave function,

$$\psi_i=\frac{1}{\sqrt{2}}\begin{pmatrix}e^{\theta_i/2}\\ e^{i\theta_i/2}\end{pmatrix}e^{i\mathbf{p}\cdot\mathbf{r}_i}. \tag{7}$$

We can now find the variational energy of this wave function, and minimize with respect to p.

The expectation value of the kinetic energy for a bond between a pair of sites is $2t_2'\Re(\psi_i^\dagger\psi_j)$. Aside from the phase factor from the momentum, this overlap is proportional to $\cos k$ for spins adjacent along the X direction (the cosine of half the angle between the spins). In particular, because the spin is conserved during the hopping, the electron cannot hop at all onto a site with an antiparallel spin. The electron kinetic energy is $2t_2\cos(p_x+p_y)+2t_2'\cos(\frac{p_x-p_y}{2})\cos k$. Minimizing over p, we obtain $\mathrm{KE}_{\min}=-2|t_2|-2|t_2'\cos(k)|$. Combining this with the previously obtained energy in the absence of t_2', Eq. (6), and minimizing with respect to ϕ and k we obtain the double spiral. This can be easily seen when the doping is very weak: focusing on the competing terms J_{2X} and $t_2'\delta$, and assuming $k\approx\frac{\pi}{2}$ to find $E=J_{2X}\cos(2k)-2t_2'|\cos k|\approx -J_{2X}+2J_{2X}(k-\frac{\pi}{2})^2-2t_2'\delta|k-\frac{\pi}{2}|$, so $|k-\frac{\pi}{2}|=\frac{t_2'\delta}{2J_{2X}}$ minimizes the energy. The incommensuration therefore is proportional to the doping strength, as observed experimentally.

If we allow the electrons to hop virtually into states that violate Hund's rule, the commensurate state survives over a finite range of dopings. When the twisting is very small, it becomes easier for an electron that is trying to hop along the antiferromagnetic diagonal to hop through the Hund's violating states than to stay in states that are parallel to the local spin but which have very small overlaps. In this case, there is no reason for the spin order to distort at all. The virtual hopping has the greater efficiency when $|t_2'\cos k|<|\frac{t_2'^2}{J_H}|$, or (using the result for k at small δ), $\delta\lesssim\frac{J_{2X}}{J_H}$. (A more detailed calculation gives the same result.) Quantum fluctuations also allow the electrons to hop more easily in this direction, by temporarily making adjacent atoms become oriented parallel to one another.

A very similar phase diagram appears for t_1 hopping. This hopping probably has weaker effects, however, since the orbital switches with each hop. This implies that an electron alternates between Hund's rule violating and satisfying states, so that the amplitude for a pair of these steps is of order $\frac{t_1^2}{J_H}$. *This* process leads to an antiferromagnetic interaction along rows and columns, but this causes incommensuration just as the ferromagnetism induced by motion along the diagonals did.

Although these calculations explain how incommensurate order can occur, the order differs from the experimentally proposed pattern in Ref. 4. The proposed order has the spin

dominantly along the $\hat{Y}$ direction whose magnitude is modulated with an incommensurate wave vector, and also a spin spiral composed of the orthogonal spin directions, at the same wave vector. While further experimental work is required to confirm the true nature of the complex incommensurate order, we note one interesting measurement, that orthorhombic symmetry is recovered at higher doping, (e.g., at $x=0.141$ [4]) where the incommensurate state is stabilized. This is consistent with our assumption that the monoclinic part of the distortion is strongly coupled to spin order. Figure 1 shows that the sense of the monoclinic distortion is correlated with the bond energies $\vec{S}_i \cdot \vec{S}_j$. Shifting the spin ordering and thus the pattern of bond energies over one site would cause the lattice to tilt in the opposite direction along the Y axis. For an incommensurate order of the kind proposed in Ref. 4, these bond energies are also modulated with an incommensurate wave vector, which removes the monoclinic distortion. In contrast, for the orders described by Eq. (5), including both the double and single spirals we have considered, the bond energies are independent of incommensuration, hence a monoclinic distortion is expected throughout. An example of a spiral order that would not induce a monoclinic distortion, close to the commensurate state of interest is two oppositely propagating spirals: $\theta_i=(-1)^{x_i+y_i}k(x_i-y_i)$, with k close to $\frac{\pi}{2}$. Effects that we have neglected, including spin anisotropy and the effect of the excess iron moments, can modify the precise form of the incommensurate state.

Phase Separation: An additional shortcoming of this explanation of the incommensurate order is that the spiral phases can be unstable to phase separation.[23] The doped electrons prefer to be segregated into high and low density regions, with different spin orders. The predictions above can still be relevant, because repulsive forces between electrons help to limit the phase separation.

Figure 7 shows the energy as a function of doping both without and with a strong *short-range* repulsion, described by adding a term $\frac{1}{2}V\delta^2$ to the energy functional. In the figure, $K=0.4$ and the other parameter values are taken from Fig. 6. A concave down portion is unstable to phase separation. For a doping in between A and B, i.e., $0.1 \leq \delta \leq 0.6$, dividing the compound up into two regions with the dopings 0.1 and 0.6 gives a state with a lower energy, whose energy is represented by the tangent. In this case, the ground state is a mixture between a doubled spiral with a low-electron density and an antiferromagnetically ordered high-density portion.

The Coulomb interactions can have one of two consequences; they either stabilize a uniform state as just described (if the force is strong enough at short distances), or else they force the two coexisting phases to fill small alternating portions of the FeTe, rather than becoming completely segregated. The ordering with alternating regions of the $(\frac{\pi}{2},\frac{\pi}{2})$ and (π,π) phases could also be incommensurate.

Additional Doping: A surprising order may arise if the compound is sufficiently doped, which would illustrate our central assumption that the orthorhombic part of the structural distortion arises from orbital, rather than spin ordering. In our model, large electron doping would drive ferromagnetic order on each of the A and B sublattices. (This optimizes the electron kinetic energy.) The sublattices continue

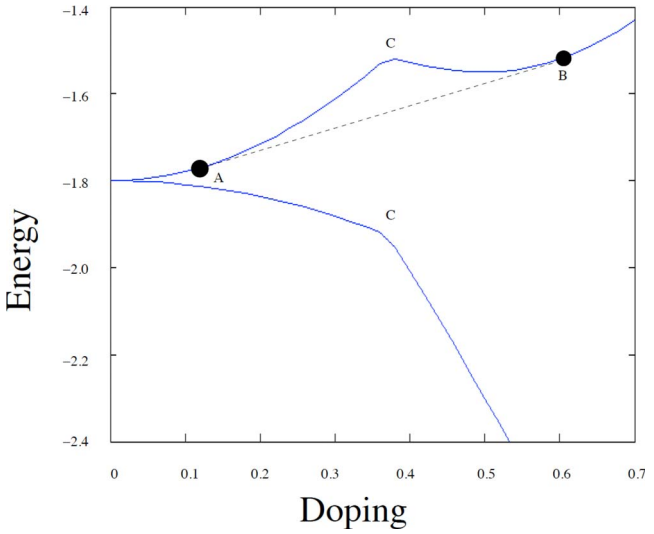

FIG. 7. (Color online) Energetics of phase separation. The solid curve shows the energy of states with uniform doping, with repulsion $V=6J_{2X}$ (upper curve) and without. The parameters are the same as in Fig. 6, with $K=0.4$. The concave down portion of each energy curve is unstable to phase separation. The points labeled C show the unphysical transition between the doubled and single-spiral states. The dashed line corrects the upper energy-curve, by showing the energy of the state where the A and B phases coexist.

to couple together antiferromagnetically, leading to (π,π) magnetic order. In Fig. 6, the order varies from commensurate, to the double spiral phase, to the (π,π) antiferromagnetic phase as the doping increases along a line at $K=0.5J_{2X}$. (For a smaller value of K, the pure spiral phase occurs before (π,π) antiferromagnetism sets in.) Note however, that while (π,π) antiferromagnetic order is compatible with tetragonal symmetry, here we expect orbital order to persist and result in an orthorhombic distortion, clearly signaling the independence of structural and magnetic order.

On the other hand, *hole* doping weakens the kinetic energy effect to the point where each sublattice has ordinary antiferromagnetic order, and the biquadratic interaction orients the two sublattice-spins parallel to each other, leading to $(\pi,0)$ magnetic order of the type seen in the FeAs materials. Again, while the $(\pi,0)$ ordering would be accompanied by compression along the x or y axis if this were magnetically driven, here, we expect the orbital ordering to remain the same, so the diagonal distortion would not change. A more direct test of whether the distortion or the magnetic ordering is the primary phenomenon is to apply a strong magnetic field to eliminate the magnetic ordering and see whether the distortion remains. This would be possible if the exchange interactions are weak, or can be weakened by modifying the compound somehow, e.g., by applying pressure.

III. TRANSPORT AND SINGLE ELECTRON PROPERTIES

The main consequence for transport of the orbital ordering-induced quasi-one-dimensionality is that the conductivity should be strongly anisotropic. Below the orbital and magnetic ordering temperature, the excess electrons in

the Yz band move much more readily in the Y direction, because t_2 is greater than t_1, t_2'. Furthermore, the spins are ferromagnetically aligned along this direction, and can hence propagate easily. To travel in the orthogonal direction, they must cross through diagonals where the spins are oppositely aligned. While a difference in electrical conductivity along the two diagonal directions is hardly surprising given the symmetry of the low-temperature state, the specific prediction here is that this will be a significant effect, and the nature of the anisotropy is that the low conductance is to be found along the antiferromagnetically ordered diagonals.

Experimentally, a Drude peak has been observed to develop below the ordering transition.[10] Since a test of anisotropy demands a single domain, optical conductivity on a sample where the domain size is larger than the spot size is required, and should be feasible. There, depending on the direction of the polarization, a different conductivity should result. More specifically, if we write $\sigma(\omega)=\frac{ne^2\tau}{m^*}\frac{1}{1+i\omega\tau}$, both the effective mass m^* and the scattering rate τ are expected to be anisotropic. The scattering rate is expected to be large in the X-direction because of scattering by incoherent spin waves,[24] a feature that is particularly prominent for low frequencies.

ARPES Given the quasi-one-dimensional dispersion along the diagonals, a narrow elliptical Fermi surface tilted at 45° to the Fe-Fe bonds is expected to appear below the ordering temperature. Moreover, these would be orbitally polarized, which can be experimentally tested using polarized light to determine orbital content along high symmetry directions. When the scattering plane containing the photon and the ejected electron is perpendicular to the surface, and along, say, the Yz plane, selection rules imply that $S(P)$ polarized light with polarization perpendicular to (parallel to) the scattering plane, ejects only electrons in the $Xz(Yz)$ orbital. The strongly dispersing part of the Fermi surface should therefore disappear for S polarized light, and will have the form shown in Fig. 8, if a single domain is imaged. The polarization dependence provides an experimental signature even from multidomain data. Current ARPES data on FeTe[9] has not reported such a signature; however, the intensity associated with this Fermi surface segment is hard to estimate reliably. Direct experimental probes of orbital ordering should also be able to test this scenario. We hope this prediction will stimulate further experiments.

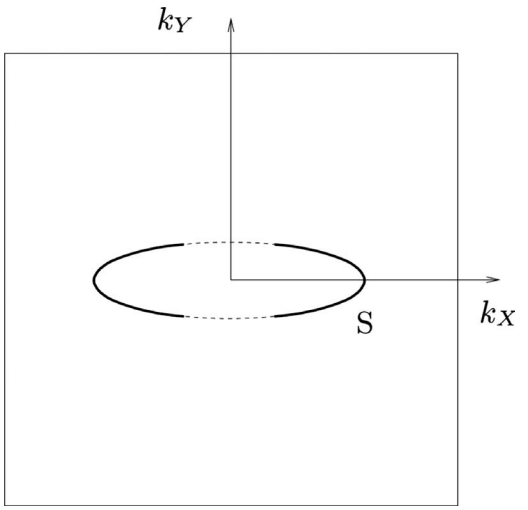

FIG. 8. The shape of the Fermi surface of the metallic electrons in the Yz orbitals, for the actual Brillouin zone. We predict that the surface is narrow in the ferromagnetic direction. Furthermore, certain parts of the ellipse should disappear in ARPES with polarized light. The dashed portions of the Fermi surface fade out for S polarization. This tests the assumption that the anisotropy results not from the lattice distortion but because the dispersing electrons are in a single orbital.

IV. CONCLUSIONS

We have argued that FeTe, a material closely related to the recently discovered Fe based superconductors, is likely to be a fairly strongly correlated material. This motivates us to use a local picture of the electronic structure, which in turn can explain, quite naturally, the unusual magnetism observed in this material. The key ingredient of this scenario is an emergent quasi-one-dimensionality arising from orbital ordering along the diagonals. While this theoretical scenario is a simplified caricature of the real system, it does make several qualitative predictions for experiments, which should be readily testable. The conductivity should be anisotropic, with higher conductivity along the ferromagnetic direction, if the unusual magnetic order is caused by the kinetic energy of conduction electrons. Certain parts of the electron Fermi surface should disappear in polarized ARPES, indicating the orbital ordering (see Sec. III for the discussion of anisotropic conductivity and ARPES). The dispersion of spin waves measured by inelastic neutron scattering should indicate ferromagnetic coupling along the Y direction (see Fig. 3). Lastly, if the Jahn Teller effect causes the orthorhombic distortion, then the distortion should persist even when the magnetic order is removed or changed to one which would not be expected to favor lattice distortion on the basis of symmetry (see the final portion of Sec. II E).

ACKNOWLEDGMENTS

We thank Eugene Demler for thoughtful conversations, and acknowledge support from LBNL DOE-504108.

[1] Y. Kamihara, T. Watanabe, M. Hirano, and H. Hosono, J. Am. Chem. Soc. **130**, 3296 (2008).
[2] W. Z. Hu, J. Dong, G. Li, Z. Li, P. Zheng, G. F. Chen, J. L. Luo, and N. L. Wang, Phys. Rev. Lett. **101**, 257005 (2008).
[3] D. Fruchart, P. Convert, P. Wolfers, R. Madar, J. P. Senateur, and R. Fruchart, Mater. Res. Bull. **10**, 169 (1975).
[4] W. Bao *et al.*, Phys. Rev. Lett. **102**, 247001 (2009).
[5] S. Li, C. de la Cruz, Q. Huang, Y. Chen, J. W. Lynn, J. Hu, Y.-L. Huang, F.-C. Hsu, K.-W. Yeh, M.-K. Wu, and P. Dai, Phys. Rev. B **79**, 054503 (2009).
[6] S. Chiba, J. Phys. Soc. Jpn. **10**, 837 (1955).
[7] The localized spin can be estimated from the Curie-Weiss law for free spins, $\chi=0.50\frac{g^2S(S+1)}{T+\Theta}$ emu/Oe-mol, (with T measured in Kelvin), where $g=2$ is the g-factor, Θ is the Curie temperature, and S is the spin. Ref. 5 fits measurements of FeTe, and obtains the "effective magneton number" $g\sqrt{S(S+1)}=2.05$ and $\Theta=130°$ K, from which we deduce $S=.64$. This is smaller than the spin in the ordered state, but the Curie-Weiss law is not exact for strong correlations. This susceptibility cannot be attributed entirely to the doped iron atoms. The 5% excess iron atoms in the sample used by Ref. 5 would have to have $S=4$ in order to contribute so much to the susceptibility.
[8] A. Subedi, L. Zhang, D. J. Singh, and M. H. Du, Phys. Rev. B **78**, 134514 (2008).
[9] Y. Xia, D. Qian, L. Wray, D. Hsieh, G. F. Chen, J. L. Luo, N. L. Wang, and M. Z. Hasan, Phys. Rev. Lett. **103**, 037002 (2009).
[10] G. F. Chen, Z. G. Chen, J. Dong, W. Z. Hu, G. Li, X. D. Zhang, P. Zheng, J. L. Luo, and N. L. Wang, Phys. Rev. B **79**, 140509(R) (2009).
[11] C. Fang, B. A. Bernevig, and J. Hu, EPL **86**, 67005 (2009).
[12] M. D. Johannes and I. I. Mazin, Phys. Rev. B **79**, 220510(R) (2009).
[13] M. J. Han and S. Y. Savrasov, Phys. Rev. Lett. **103**, 067001 (2009).
[14] F. Krüger, S. Kumar, J. Zaanen, and J. van den Brink, Phys. Rev. B **79**, 054504 (2009).
[15] R. R. P. Singh, arXiv:0903.4408 (unpublished).
[16] W. Lv, J. Wu, and P. Phillips, arXiv:0905.1704 (unpublished).
[17] W. Malaeb *et al.*, J. Phys. Soc. Jpn. **77**, 093714 (2008).
[18] P. A. Lee and X. G. Wen, Phys. Rev. B **78**, 144517 (2008).
[19] Y. Ran, F. Wang, H. Zhai, A. Vishwanath, and D.-H. Lee, Phys. Rev. B **79**, 014505 (2009).
[20] C. Xu and J. Hu, arXiv:0903.4477 (unpublished).
[21] F. Ma, W. Ji, J. Hu, Z.-Y. Lu, and T. Xiang, Phys. Rev. Lett. **102**, 177003 (2009).
[22] O. Madelung, *Introduction to Solid-State Theory* (Springer-Verlag, Berlin, 1996).
[23] E. Dagotto, T. Hotta, and A. Moreo, Phys. Rep. **344**, 1 (2001).
[24] See e.g., C. L. Kane, P. A. Lee, and N. Read, Phys. Rev. B **39**, 6880 (1989).